Differences in protein mobility between pioneer versus follower growth cones

Rajan P. Kulkarni*†, Magdalena Bak-Maier†‡, and Scott E. Fraser*†§

*Option in Biochemistry and Molecular Biophysics, †Division of Biology, California Institute of Technology, Pasadena, CA 91125

Communicated by Harry B. Gray, California Institute of Technology, Pasadena, CA, November 15, 2006 (received for review May 10, 2006)

Navigating growth cones need to integrate, process and respond to guidance signals, requiring dynamic information transfer within and between different compartments. Studies have shown that, faced with different navigation challenges, growth cones display dynamic changes in growth kinetics and morphologies. However, it remains unknown whether these are paralleled by differences in their internal molecular dynamics. To examine whether there are protein mobility differences during guidance, we developed multiphoton fluorescence recovery after photobleaching methods to determine molecular diffusion rates in pathfinding growth cones *in vivo*. Actively navigating growth cones (leaders) have consistently longer recovery times than growth cones that are fasciculated and less actively navigating (followers). Pharmacological perturbations of the cytoskeleton point to actin as the primary modulator of diffusion in differently behaving growth cones. This approach provides a powerful means to quantify mobility of specific proteins in neurons *in vivo* and reveals that diffusion is important during axon navigation.

cytoplasmic dynamics | neuronal migration | two-photon microscopy | zebrafish

The initial wiring of the vertebrate brain involves a small number of neuronal cell clusters and the axons connecting them (1–3). Wiring this initial network of nerve cells involves guided extension of axons, led by their navigating tips called growth cones, toward their final targets (4). In many cases, leader growth cones (pioneers) trail-blaze the initial paths actively sensing guidance cues as they grow; follower axons largely progress along the leaders' tracks, simplifying their navigation challenges to more constrained explorations of their local environments (5). The different navigation schemes used by pioneers and followers are reflected in the differences in their external morphologies and behavior (5–9). However, we do not know whether similar differences might also exist inside the growth cones, reflected in differences in protein mobility. Neither the kinetics of local protein movement nor the effects of cytoskeletal elements on protein mobility have been probed in growth cones *in vivo*. Localized diffusion differences in growth cones may be critical for the delivery or relocalization of molecular species into the growth cone tip, thus influencing the strength and extent of signaling cascades induced by activated guidance receptors and on cytoskeleton regulation associated with growth cone motility and guidance.

Diffusion through a viscous medium such as the cytoplasm can be affected by a number of factors, including the local and global tortuosity of the cytoplasm, interactions between species, and complex formation. Local tortuosity refers to the microenvironment around which the protein species has to diffuse; this can be increased by greater cross-linking or turnover of actin. Global tortuosity deals with the geometry of the entire cytoplasmic space, including the cell membrane. Cells with multiple membrane invaginations would have slower diffusion rates compared with those with smoother contours. Interactions between proteins will cause the apparent diffusion constant to be smaller than expected as there will be a finite interaction time. Alternately, permanent complex formation can reduce the diffusion rate by increasing the effective radius. For noninteracting proteins such as GFP, the local tortuosity of the cytoplasm will likely have the most significant effect on diffusion rate. Cell regions with increased density would have slower protein diffusion rates, resulting in longer transient contacts for recognition. For proteins in the cytoplasm, an increase in interaction time could affect signaling processes, thereby leading to different transcription rates or events and thus potentially affecting aspects of development.

In the present study, we developed a method for examining the dynamics of protein diffusion in developing neurons of live zebrafish embryos using one- and two-photon fluorescence recovery after photobleaching (FRAP) at selected time intervals during development. FRAP has been used to study the mobility, transport, and subcellular organization of fluorescently tagged molecular species in cultured cells (10–15) but rarely in a three-dimensional embryo. In FRAP, a small region is bleached using high-intensity laser illumination; the recovery of fluorescence by diffusion of nonbleached fluorescent molecules into this area from the mobile fraction is then monitored using low-intensity illumination. Because recovery depends on the movement of unbleached fluorophores from the surrounding areas, we can calculate a diffusion constant, D, for those molecules (13, 16–18).

We have previously described the formation of the postoptic commissure (POC), a commissural axon tract connecting the ventro-rostral clusters of neurons across the midline in the zebrafish forebrain (5) (Fig. 1*a*). A stable transgenic line of zebrafish using the gata2::GFP highlights the cluster of neurons that establish the POC (19). These clusters make up an equivalence group of cells where the axon of one cell can substitute for another (followers can become leaders) (5). Using time-lapse imaging, followers can be observed while they grow along leaders and when they detach from them and grow on their own allowing us to test for any differences in growth cones that might exist during these different navigation modes. Here, we combine FRAP measurements with time-lapse analysis to explore the relationship between protein mobility and growth cone guidance by measuring the dynamics of cytoplasmic diffusion in early neurons and their growth cones. The results allow us to correlate regional diffusion measurements with growth cone behavior as POC axons establish the early commissural tract in a living embryo and test for linkage. This approach can be used to quantitate other intracellular dynamics within the developing vertebrate embryo, thus providing a powerful tool for analyzing

Author contributions: R.P.K., M.B.-M., and S.E.F. designed research; R.P.K. and M.B.-M. performed research; R.P.K. contributed new reagents/analytic tools; R.P.K. and M.B.-M. analyzed data; and R.P.K., M.B.-M., and S.E.F. wrote the paper.

The authors declare no conflict of interest.

Abbreviations: FRAP, fluorescence recovery after photobleaching; POC, postoptic commissure; hpf, hours postfertilization.

‡Present address: University of Bristol, Bristol BS8 1TD, United Kingdom.

§To whom correspondence should be addressed. E-mail: sefraser@caltech.edu.

This article contains supporting information online at www.pnas.org/cgi/content/full/0610142104/DC1.

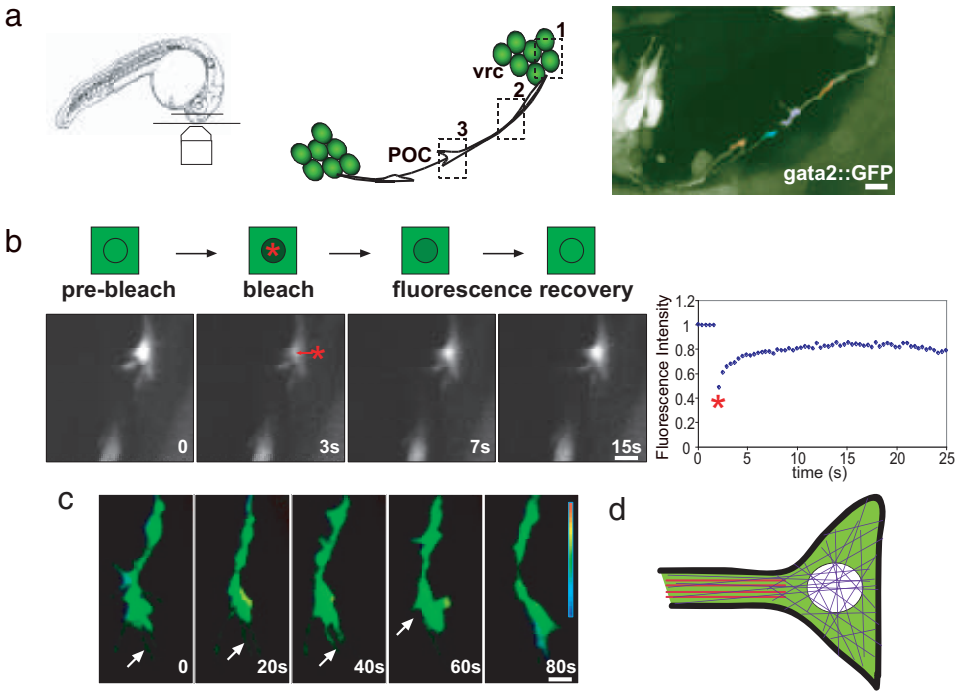

Fig. 1. Single and two-photon FRAP analysis. (*a*) (*Left*) Schematic showing embryo preparation for imaging and FRAP analysis. (*Center*) Diagram of the postoptic commissure (POC) axon tract showing the three regions of the gata2::GFP neurons where FRAP measurements were taken: (1) cell body, (2) axon process, and (3) growth cone. Ventro-rostral cluster (vrc). (*Right*) A 23-hpf gata2::GFP embryo showing GFP positive vrc cells and early POC axons growing to midline. Individual POC growth cones have been highlighted by color. Black regions correspond to nonfluorescing cells. (Scale bar, 2 μm.) (*b*) The image sequence represents a typical FRAP experiment performed on a leader growth cone. Prebleach sequences are acquired to provide baseline fluorescence, followed by the bleach (asterisk). Fluorescence recovery is then recorded and can be plotted as shown on the right. (Scale bar, 2 μm.) (*c*) Depth-coded *z* stack of a leader growth cone showing no significant change in the axial position of the growth cone during the length of a typical FRAP experiment. Arrows indicate filopodia. (Scale bar, 2 μm.) (*d*) Cartoon of growth cone showing relative size of growth cone, axon terminus, and bleach spot. GFP recovery occurs from regions within the growth cone but outside the bleach spot. Bleach spot is 1 μm in diameter. Actin filaments are shown in blue, microtubules are shown in red. For clarity, filopodial projections are not shown.

functional relationships between cellular behaviors and protein dynamics.

Results

Protein Diffusion in Small Cellular Compartments *in Vivo*. As a reporter of intracellular protein mobility, we used the gata2::GFP transgenic line, which expresses GFP in neurons and measured the diffusion rates of GFP in different regions of young neurons (Fig. 1*a*) with both one and two-photon FRAP microscopy. The high level of GFP expression allows the behavior of early POC axons and their growth cones to be observed *in vivo* as they navigate across the midline and interact with their surroundings and each other (5) (Fig. 1*a*). These neurons first begin growing out at 21 h and finish at ≈24 h. Therefore, we first examined the diffusion of cytosolic gata2:GFP-expressing vrc neurons at 22–24 h postfertilization (hpf) GFP in three main neuronal compartments: the cell body, the axon process and the growth cone (Fig. 1*a*, $n = 60$ separate embryos). We analyzed lateral diffusion rates based on fluorescence recovery traces obtained from two-dimensional scans over time [Fig. 1*b*, also see supporting information (SI) Fig. 4 and Movies 1–3 for sample bleach sequences). Due to the large nucleus, the cytoplasmic volume in early neurons is small, effectively reducing the cytoplasm to two-dimensions and thus allowing comparison of diffusion among the compartments (see *SI Text*).

The FRAP measurements require that active structures such as growth cones remain in the same axial plane (*z* dimension) to ensure that changes in the signal do not result because of sample movement out of the focal plane. To assess the axial mobility of growth cones, we used depth-coded *z* stacks of the same growth cone at different time-points. Four-dimensional (*x*, *y*, *z*, and time) time-lapse movies of early POC growth cones showed that early growth cones remain in the same axial plane for up to 2 min, which is sufficient time for FRAP measurements (Fig. 1*c*). During this time, POC growth cones actively sample their environment as revealed by the appearance and disappearance of individual filopodia (Fig. 1*c*, arrows). Postbleach traces in the three compartments (cell body, axon process, growth cone) showed rapid recovery, occurring on the order of seconds (Fig. 2 *a–c*), with diffusion being fastest in the cell body and slowest in the growth cone (Table 1). Control experiments using fixed gata2::GFP embryos showed no recovery as expected (not shown). The observed diffusion was neither affected by GFP expression levels nor specific to the vrc cells. FRAP measurements yielded similar diffusion rates when using the islet1::GFP transgenic line (20), which has lower GFP expression at this stage compared with the gata2::GFP fish, as well as when examining neurons belonging to the dorsorostral cluster in slightly older gata2::GFP embryos (27 hpf). [Diffusion values were $D = 0.94 \pm 0.07$ μm^2/s in islet::GFP positive neurons and $D = 0.96 \pm 0.15$ μm^2/s in neurons of the dorso-rostral cluster in the gata2::GFP line.]

To confirm that the observed GFP diffusion kinetics could be replicated by another similar-sized molecule, we examined the kinetics of YFP. To do this, we used gata2::GFP embryos injected with YFP mRNA and compared the GFP/YFP diffusion values; in these embryos, YFP is expressed at a significantly lower level than GFP. For this experiment we used two-photon FRAP, allowing us to examine GFP/YFP recovery kinetics simultaneously. We obtained virtually identical fluorescence

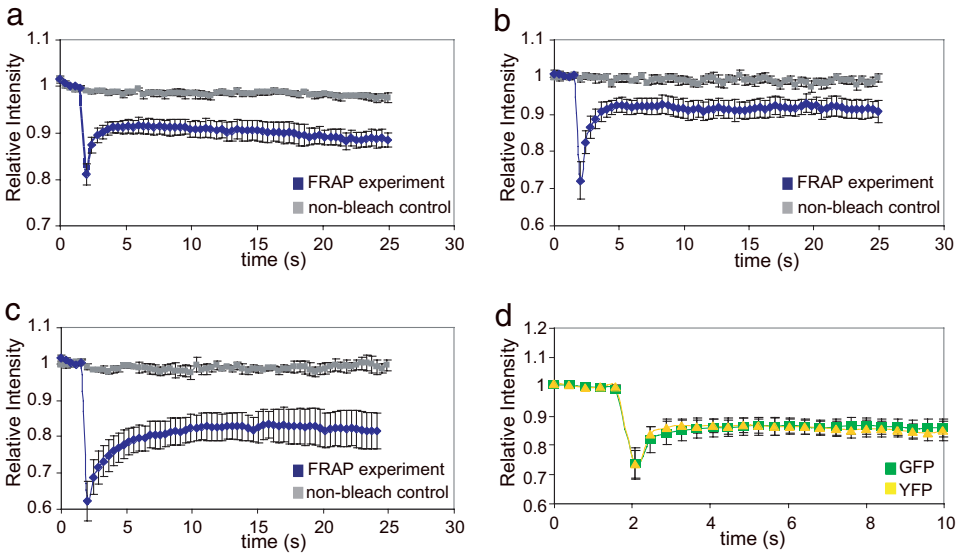

Fig. 2. Average fluorescence recovery traces obtained with either single or two-photon FRAP imaging in different compartments of young neurons *in vivo*. (*a*) Cell body. (*b*) Axon process. (*c*) Leader growth cone. The nonbleached control for each compartment is plotted in gray. (*d*) YFP/GFP cell-body two-photon comparison. The YFP average trace was normalized to the GFP.

recovery traces (Fig. 3*d*) and diffusion values for both fluorescent species [0.92 ± 0.16 μm^2/s (GFP), 0.94 ± 0.17 μm^2/s (YFP); $n = 15$]. The mobile fraction, which refers to the fraction of cytoplasmic protein that is free to diffuse (i.e., not bound or associated with internal structures) and therefore contribute to fluorescence recovery, was similar for both GFP and YFP, suggesting that both species are able to travel with the same degree of freedom inside the cell and thus are good reporters of diffusion in early neurons for other proteins of similar sizes. As the diffusion values for GFP and YFP obtained using two-photon FRAP are similar to the one-photon results obtained earlier (Table 1), we concluded that, for this experiment, out-of-focus light did not significantly perturb diffusion measurements. Two-photon illumination permits deeper penetration into the sample and reduced radiation outside of the focal plane of the laser beam, significantly reducing bleaching in the axial direction. Thus, two-photon FRAP might be the method of choice for studying protein mobility in older or deeper tissues.

Leaders Have Slower Diffusion Kinetics than Followers. To determine whether differences between leader and follower growth cones are reflected in cytoplasmic diffusion rates, we compared GFP diffusion in the two growth cone types. Analyses of three-dimensional stacks revealed that the two types of growth cones have similar volumes, allowing us to directly compare FRAP measurements between the two. Leader growth cones consistently showed longer recovery times, whereas follower growth cones had rapid recoveries. The typical recovery time of the leader growth cone was 6–8 s compared with 3–4 s for a follower growth cone. Thus, GFP diffusion was significantly slower in leader growth cones (0.28 μm^2 s^{-1}, Table 1 and SI Fig. 5*a*) compared with follower growth cones (0.55 μm^2 s^{-1}); both values were unchanged irrespective of growth cone position along the commissural tract.

The clear difference in diffusion kinetics between leaders and followers led us to ask whether diffusion rate depended on axon fasciculation as this result suggested. To test this directly, we next examined off-tract follower growth cones, those that occasionally detach from other POC axons and navigate on their own. Once detached, such growth cones must pathfind as leaders or rejoin other axons to cross the midline. FRAP measurements revealed a striking decrease in GFP mobility in off-tract growth cones compared with regular follower growth cones. Off-tract growth cones had the slowest recovery, with recovery times of 12–15 s and an average diffusion of 0.15 μm^2 s^{-1} (Fig. 3*a*, Table 1, and SI Fig. 5*a*). This slow recovery time is consistent with the notion that the need to pathfind independently is reflected through cytoplasmic diffusion rates.

Table 1. GFP diffusion rates in different neuronal compartments and growth cones

	Wild type			Cytochalasin B			Nocodazole		
	N	*D* (μm^2/s)	SD	*N*	*D* (μm^2/s)	SD	*N*	*D* (μm^2/s)	SD
Leader G.C.	20	0.28*	0.11	27	0.67†	0.19	17	0.32	0.11
Follower G.C.	22	0.55*	0.27	23	0.67	0.23	34	0.54	0.20
Off-tract G.C.	9	0.15*	0.05	16	0.37†	0.17	17	0.21	0.11
Axon	23	0.71*	0.16	19	0.87†	0.21	21	0.90†	0.21
Cell Body	29	0.96*	0.22	8	0.94	0.18	9	1.12	0.18

Diffusion coefficients for GFP in various compartments of the developing zebrafish neurons are listed above. For examining the effects of actin and microtubule networks, zebrafish were injected either with cytochalasin B or nocodazole, and the diffusion coefficients for GFP were measured by region. The *P* values were generated by comparing across wild-type compartments for differences in diffusion (*, $P < 0.05$, ANOVA followed by Tukey–Kramer multiple comparison test). The effect of cytochalasin B or nocodazole on diffusion for each compartment was compared with wild type using Student's *t* test with $P < 0.05$ noted (†). G.C., growth cone.

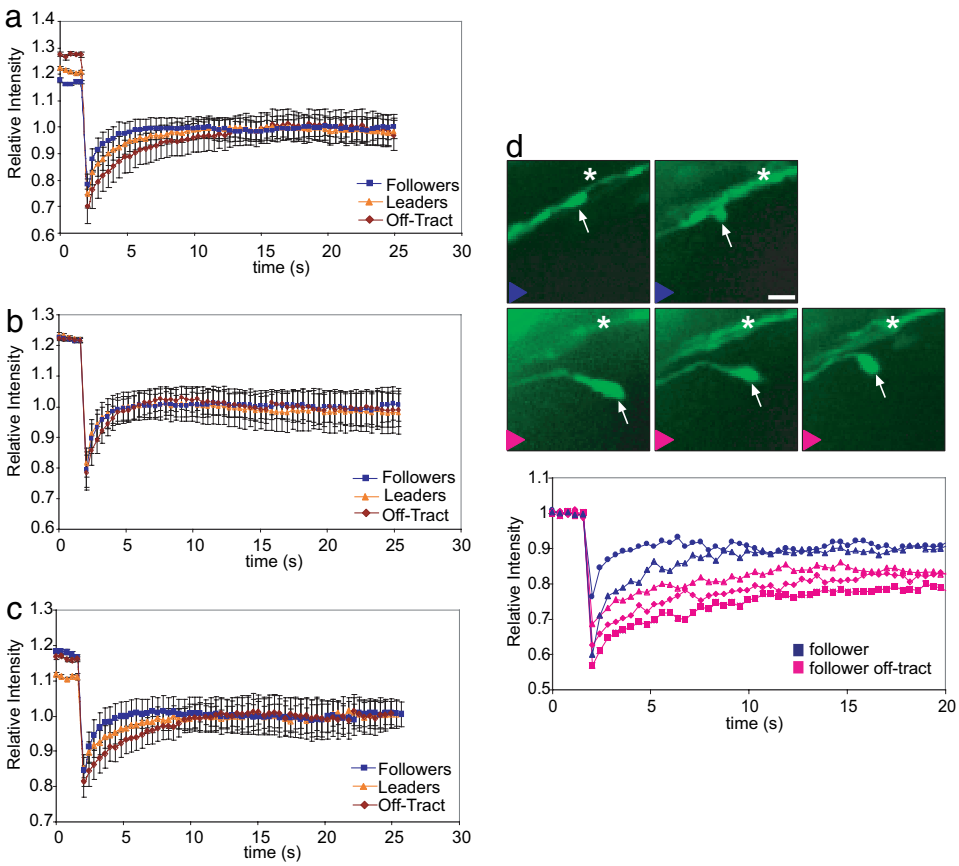

Fig. 3. Measurement of diffusion in growth cones. (*a*) Average fluorescence recovery traces in follower, leader, and follower off-tract wild-type growth cones. All traces have been normalized to the final recovery level after bleaching to illustrate the differences in diffusion kinetics. (*b* and *c*) Effects of cytochalasin B (*b*) and nocodazole (*c*) on GFP diffusion in growth cones as assayed by FRAP analysis. (*d*) Dynamic differences in GFP diffusion visualized in a single follower growth cone (arrow) as it either associates with other POC axons (asterisk) or grows away from them. Fluorescence recovery traces corresponding to these events are plotted below. Blue traces correspond to growth cone in contact with the POC axons, pink traces when the growth cone traveled away from the POC. (Scale bar, 2 μm.)

To confirm that differences in diffusion rate in growth cones were dynamically linked to the degree of interaction with the local environment versus to axon-axon interactions, we assayed the same follower growth cone as it grew away from or along other axons using time-lapse analysis and FRAP (Fig. 3*d*). Fluorescence recovery was slow at all points when the follower growth cone lost contact with other axons (Fig. 3*d*, pink lines). Both before losing contact and after reestablishing contact, recovery was rapid and the diffusion constant was similar to regular follower growth cones (those that grow along the leader axon) (Fig. 3*d*, blue lines). These experiments indicate a strong correlation between GFP diffusion and axon interactions during pathfinding. Growth cones in axons that independently probe their environments have significantly slower diffusion values compared with growth cones that wrap around other axons.

Differences Between Leaders and Followers Depend on the Actin Cytoskeleton. The observed differences in GFP mobility suggest the presence of a diffusion restriction, likely due to a cytoskeletal structure limitation. This restriction is either more extensive or longer lasting in the particular growth cones that have slower measured diffusion rates. Previous measurements have shown that the actin network can slow diffusion of long-chain dextrans in cultured neurons (21). The leading edge of the growth cone contains a meshwork of actin bundles that project radially into the filopodia (22). Cytochalasins are well characterized actin depolymerizing agents (23, 24) used to study the effects of the actin network on diffusion in systems ranging from *Dictyostelium* to cultured neurons (25, 26). To examine whether the actin network affects diffusion in the growth cone, we assayed the resulting GFP fluorescence recovery after cytochalasin B treatment. After twenty minutes, growth cones in embryos injected with cytochalasin B began to lose filopodia and became less motile compared with uninjected embryos but had similar morphologies and volumes. Cytochalasin B significantly increased the diffusion rate in both leader and off-tract growth cones (see histograms in Fig. 5*b*), which resulted in all growth cones having similar recovery kinetics (Fig. 3*c* and Table 1). Similar results were obtained with latrunculin A, another actin depolymerizing agent (data not shown). The observed increase in GFP mobility upon actin depolymerization suggests that actin plays a role in modulating local diffusion in growth cones *in vivo*.

To further elucidate the mobility of actin, we examined the diffusion and recovery kinetics of YFP-actin in leader versus follower growth cones. The YFP-actin exists in both a filamentous, polymerized form, and a freely diffusible globular form. As expected, we see a slight reduction in diffusion between GFP versus YFP-actin because the polymerized actin cannot rapidly recover when bleached. YFP-actin diffusion values were $\approx$10% slower than for pure GFP, mostly reflecting the presence of polymerized actin that is slower to turn over. However, the major difference between leaders and followers can be seen in the mobile fraction (R) of YFP-actin (Table 2). For followers, we found R to be 48.8 $\pm$ 13.2%, whereas it was 60.9 $\pm$ 10.9% in

Table 2. GFP and YFP-actin diffusion rates and recovery fractions in leader and follower neurons

	Leader G.C. ($n = 17$)	Follower G.C. ($n = 19$)
GFP diffusion, $\mu m^2/s$	0.31 ± 0.17*	0.60 ± 0.19
GFP mobile fraction, %	64 ± 11*	52 ± 13
YFP-actin diffusion, $\mu m^2/s$	0.28 ± 0.14*	0.54 ± 0.17
YFP-actin mobile fraction, %	61 ± 11*	49 ± 13

Diffusion coefficients and mobile fractions for YFP-actin in leader and follower growth cones are listed above (*, $P < 0.05$). The P values were generated by comparing measurements between leaders and followers using Student's t test.

leaders. The increase in recovery fraction between the two indicates that there is a greater mobile pool of YFP-actin in leaders versus followers, which may result from greater turnover, even though the time scale of recovery is slower. This indicates that leader growth cones experience greater polymerization and depolymerization of YFP-actin as compared with followers; the increased turnover results in a greater quantity of YFP-actin that is free to diffuse and recover fluorescence after the bleach. Indeed, overall protein turnover is also greater in leaders, as evidenced both by this and the GFP turnover data. These results, along with the observed increase in GFP mobility upon actin depolymerization in leaders, strongly suggest that actin plays a role in modulating local diffusion in growth cones *in vivo*.

The microtubule scaffold is the other important cytoskeletal network in the central region of the growth cone and axon process and is used for organelle transport and structural integrity (22). To determine how this network affects diffusion in growth cones, we treated the embryos with nocodazole, a drug that depolymerizes microtubules and is effective for microtubule destabilization in zebrafish (27). Nocodazole treatment caused progressive growth cone collapse. The growth cone remained within the axial depth of the bleach spot. However, fluorescence recovery traces did not reveal a significant effect on either recovery times or diffusion values although small decreases did occur (Fig. 3*d*, Table 1, and SI Fig. 5*c*), suggesting that the microtubule network does not play a major role in modulating local diffusion rates in growth cones *in vivo*. The nocodazole result is insightful, however, as it provides direct evidence that diffusion rate in the growth cone is not directly linked to growth cone shape *in vivo*, which, until this experiment, was a distinct possibility.

Discussion

Quantitative One- and Two-Photon FRAP Measurements *in Vivo*. The results described above demonstrate that *in vivo* FRAP can elucidate rapid context-dependent changes in diffusion and transport kinetics for molecules and complexes within developing neurons in the developing embryo. These methods allow for both qualitative and quantitative analysis of macromolecular transport parameters that can in turn be directly linked to cellular behaviors. Specifically, here we demonstrate this by measuring GFP diffusion kinetics in young neurons and show that these kinetics are not only different between the main neuronal compartments (cell body, axon, and growth cone) but also that they differ depending on the level of active pathfinding. Both one- and two-photon FRAP can be used for sensitive measurements of protein diffusion in small compartments, down to the diffraction limited laser spot size. Furthermore, the laser pulses do not significantly physically damage the embryos, as the examined cells continue to grow normally. Indeed, the same cell can be repeatedly examined by FRAP with no observable behavioral defects.

The benefits of two-photon FRAP include the ability to penetrate deeper into tissues (up to ≈500 μm), reduced radiation outside of the focal plane of the beam, and the broad spectral absorption of many common fluorophores. Because of this broad excitation maxima, there are many potential wavelengths that can be used to excite a given dye molecule, which can allow for photobleaching of multiple species simultaneously, if desired, as demonstrated here with the GFP/YFP bleach experiments. An optimal excitation wavelength can thus be identified which allows for maximal fluorophore excitation while avoiding two photon damage of sensitive intracellular structures (such as pigment granules). This study establishes the feasibility of multiphoton FRAP within the living embryo and will allow for quantitation of additional developmental events. The broad applicability of this technique toward many different cell types and fluorophores of choice marks a significant step in the ability to probe the dynamics of biological systems *in vivo*.

Protein Dynamics in Growth Cones. Our results demonstrate notable differences in internal diffusion dynamics of *in vivo* growth cones when they face different navigation challenges. Cytoplasmic diffusion rates are slower when growth cones are actively navigating, whether they are true leaders or off-tract followers. Specifically, the observed differences in GFP mobility suggest the presence of transient diffusion restrictions within the neuronal cytoplasm; perturbation of the actin and tubulin networks point to actin as the primary modulator of the diffusion differences. Depolymerization of actin abolished differences in GFP mobility among the different growth cone types, whereas depolymerization of tubulin did not. The leading edge of the growth cone is actin-rich; as the growth cone navigates through its environment, there is significant turnover of this actin.

The organization and rearrangement of the cytoskeleton have long been known to play critical roles in growth cone motility and navigation. Cytoskeletal processes underlie the constant flux within the growth cone, including surface presentation of guidance receptors and new protein synthesis/delivery (28). In the simplest scenario, this suggests that, in addition to external differences in morphology between leader and follower growth cones, the intracellular cytoskeletal structures might also be different. The YFP-actin results indicate that leaders have a more elaborate cytoskeleton. The finding that off-tract followers resemble leaders in their diffusion characteristics suggests a dynamic link between the actin network and guidance signaling that can alter internal growth cone structure and diffusion rates.

Recently, specific guidance cues have been shown to directly affect the actin and microtubule cytoskeletons (29). An interesting possibility is that, in addition to its role in mobility, the actin network in growth cones sets up transient boundaries that effectively limit diffusion on time scales that temporally affect delivery and local concentrations of molecules critical for growth. The actin network creates a mesh with a given pore size; changing the pore size of the actin cytoskeleton may be important for mobility and dynamic organization of the neuron. Such control of the actin network could serve as a mechanism for amplifying local guidance signals, helping growth cones navigate, and ultimately controlling nervous system wiring and development.

In the present stage of developmental neurobiology, we are increasingly more interested not only in the function of proteins but also their mobilities and understanding how these processes are interrelated. Until now, however, such studies have been largely restricted to *in vitro* systems. The approach shown here is an exciting step forward in our ability to directly observe and measure protein movement in cells of living embryos.

Methods

Fish Maintenance. Raising and spawning of adult zebrafish were performed as outlined in the Zebrafish Book (30) and in

accordance with the animal care guidelines of the California Institute of Technology.

Embryo Preparation and Imaging Details. ***Embryo preparation and pharmacological treatments.*** Embryos at 20–22 hpf were anesthetized with tricaine (0.01%) and embedded in a drop of 1.2% ultralow melt agarose on a coverslip-bottom Petri dish in 30% danieau/0.01% tricane/0.15 mM phenylthiourea. Pharmacological inhibitors of the cytoskeleton were injected into the neural tube of embryos between 18–24 hpf, and embryos recovered for 10–20 min at 28°C. Nocodazole (Sigma, St. Louis, MO) was used at a concentration of 20–40 μM and cytochalasin B (Sigma) was used at 4 μg/ml. Embryos were mounted in an inverted position to allow imaging of commissural axons. Injected embryos were imaged 30 min after injection.

Imaging details. All imaging was performed using an inverted Zeiss 510Meta Confocal Microscope with a Plan-Neofluar 40×/NA 1.3 objective. Temperature was maintained at 28–29°C throughout experiments. GFP-positive cells were excited with a 30 mW 488-nm argon laser with a 505LP Chroma filter and a pinhole setting of 1.5–2.0 Airy units. The interval between consecutive images was 390 ms.

FRAP Measurements and Analysis. One hundred images (512 × 512) were acquired in continuous time-lapse mode. Five images were acquired before the bleach to obtain a baseline. For *in vivo* experiments, a circular region, 1 μm in diameter, was defined and bleached at full laser power (100% transmission, five to seven pulses). Fluorescence recovery was monitored by scanning the whole field at low power (1–2% transmission), and the intensity recovery traces were recorded. The bleaching characteristics of the laser were determined by bleaching a spot in an immobile specimen of fluorescein using the same laser and objective settings. Under these conditions, GFP and fluorescein quenching are similar (31). From this data, the beam profile and $1/e^2$ beam radius were determined. Diffusion coefficients for GFP were determined by classical FRAP analysis, as described (16, 17, 32). The fluorescence of the entire bleach spot was measured to generate recovery traces and analysis performed as described in *SI Text*.

Two-Photon FRAP Measurements and Analysis. Diffusion coefficients for GFP and YFP were determined by two-photon FRAP analysis, as described (33). Two-photon FRAP measurements were performed using a Zeiss LSM510 META microscope with a Coherent Chameleon two-photon Ti:sapphire laser. Both GFP and YFP were simultaneously bleached using 900-nm light with a 40×/NA 1.3 Apochromat objective. Cell body compartment was chosen based on the YFP expression being strongest in this region. The bleaching characteristics of the laser were determined by bleaching a spot in an immobile specimen of fluorescein using the same laser and objective settings as for *in vivo* imaging. From this data, the $1/e^2$ axial (w_z) and radial (w_r) beam dimensions were determined.

For all two-photon experiments, a circular region 1.4 μm in diameter was defined and photobleached at full power (100% power, 100% transmission, seven to nine pulses) and fluorescence recovery monitored by scanning the whole field of interest at low laser power after the bleach (100% power, 10% transmission). The fluorescence intensity recovery traces were recorded and analysis was performed as described in *SI Text*.

Data Analysis. The D coefficients for each category were compared for significance using GraphPad (San Diego, CA) InStat 3.0. In cases where control diffusion rate was compared with more than one perturbation, the P value was recalculated to adjust for multiple comparisons. Values of $P < 0.05$ were considered statistically significant.

We thank Michael Liebling, Helen McBride, and Marianne Bronner-Fraser for helpful discussion and comments on the manuscript. This work was supported by the Beckman Institute at Caltech and National Institutes of Health Grants HD043897 and HD037105 (to S.E.F.) and a National Defense Science and Engineering Graduate Fellowship (to R.P.K.).

1. Chitnis AB, Kuwada JY (1990) *J Neurosci* 10:1892–1905.
2. Mastick GS, Easter SS, Jr (1996) *Dev Biol* 173:79–94.
3. Wilson SW, Ross LS, Parrett T, Easter SS, Jr (1990) *Development (Cambridge, UK)* 108:121–145.
4. Tessier-Lavigne M, Goodman CS (1996) *Science* 274:1123–1133.
5. Bak M, Fraser SE (2003) *Development (Cambridge, UK)* 130:4999–5008.
6. Bovolenta P, Dodd J (1990) *Development (Cambridge, UK)* 109:435–447.
7. Bovolenta P, Mason C (1987) *J Neurosci* 7:1447–1460.
8. McConnell SK, Ghosh A, Shatz CJ (1989) *Science* 245:978–982.
9. Myers PZ, Bastiani MJ (1993) *J Neurosci* 13:127–143.
10. Cheutin T, McNairn AJ, Jenuwein T, Gilbert DM, Singh PB, Misteli T (2003) *Science* 299:721–725.
11. Coscoy S, Waharte F, Gautreau A, Martin M, Louvard D, Mangeat P, Arpin M, Amblard F (2002) *Proc Natl Acad Sci USA* 99:12813–12818.
12. Festenstein R, Pagakis SN, Hiragami K, Lyon D, Verreault A, Sekkali B, Kioussis D (2003) *Science* 299:719–721.
13. Lippincott-Schwartz J, Snapp E, Kenworthy A (2001) *Nat Rev Mol Cell Biol* 2:444–456.
14. Nehls S, Snapp EL, Cole NB, Zaal KJ, Kenworthy AK, Roberts TH, Ellenberg J, Presley JF, Siggia E, Lippincott-Schwartz J (2000) *Nat Cell Biol* 2:288–295.
15. Phair RD, Misteli T (2000) *Nature* 404:604–609.
16. Axelrod D, Koppel DE, Schlessinger J, Elson E, Webb WW (1976) *Biophys J* 16:1055–1069.
17. Klonis N, Rug M, Harper I, Wickham M, Cowman A, Tilley L (2002) *Eur Biophys J* 31:36–51.
18. White J, Stelzer E (1999) *Trends Cell Biol* 9:61–65.
19. Meng A, Tang H, Ong BA, Farrell MJ, Lin S (1997) *Proc Natl Acad Sci USA* 94:6267–6272.
20. Higashijima S, Hotta Y, Okamoto H (2000) *J Neurosci* 20:206–218.
21. Popov S, Poo MM (1992) *J Neurosci* 12:77–85.
22. Dent EW, Gertler FB (2003) *Neuron* 40:209–227.
23. Brown SS, Spudich JA (1981) *J Cell Biol* 88:487–491.
24. Flanagan MD, Lin S (1980) *J Biol Chem* 255:835–838.
25. Forscher P, Smith SJ (1988) *J Cell Biol* 107:1505–1516.
26. Potma EO, de Boeij WP, Bosgraaf L, Roelofs J, van Haastert PJ, Wiersma DA (2001) *Biophys J* 81:2010–2019.
27. Solnica-Krezel L, Driever W (1994) *Development (Cambridge, UK)* 120:2443–2455.
28. Campbell DS, Holt CE (2001) *Neuron* 32:1013–1026.
29. Gallo G, Letourneau PC (2004) *J Neurobiol* 58:92–102.
30. Westerfield M (1993) *The Zebrafish Book* (Univ of Oregon Press, Eugene).
31. Swaminathan R, Hoang CP, Verkman AS (1997) *Biophys J* 72:1900–1907.
32. Koppel DE, Axelrod D, Schlessinger J, Elson EL, Webb WW (1976) *Biophys J* 16:1315–1329.
33. Brown EB, Wu ES, Zipfel W, Webb WW (1999) *Biophys J* 77:2837–2849.